LOCAL AND DISTRIBUTION ANALYSIS OF METALS AND ALLOYS

By

J. GIBER, I. V. PERCZEL, F. PAVLYÁK and B. ALBERT*

Institute of Physics, Technical University, Budapest
* Csepel Iron and Metal Works, Budapest
Received April 16, 1980

I. Introduction

In recent times, it is ever more generally recognized and supported by experience, also in this country, that no unambiguous relation can be established from the composition data obtained by the methods of concentration analysis between the composition and the properties of the material under examination. For instance, the measured mechanical properties elasticity [1] and strength [2] of aluminium alloys with the same average composition are very different.

Likewise, there are data demonstrating that the conventional methods are not satisfactory to follow with a sufficient accuracy the amounts and distribution of nonmetallic impurities and additives similarly affecting the properties of alloys.

Consequently a deliberate and reproducible production of alloys requires up-to-date, high sensitivity local analytical methods covering the complete range of the main components, additives and impurities, at the same time:

1. suit for concentration analysis with special regard to nonmetallic impurities (O, H, B) and to the ppm concentration ranges;

2. supply information on the distribution to a depth of several μm with a depth resolution of a few nm, and thus, determine the surface and interface layer structures;

3. suit for determining the lateral distribution of the components according to section 1 with a lateral resolution of μm, and in other cases of a few hundred μm, order thus permitting to study the grain boundaries, precipitations, enrichments and segregations;

4. suit for localization connected to the topography of the composition analysis and new reproducible measurements at any time;

5. detect the local coordination and the chemical bond;

6. make possible absolute and relative quantitation.

Table 1

Method	Type and manufacturer of the equipment pieces	Range of examinations	Sensitivity	Lateral resolution	Depth resolution	Special possibilities
SIMS	BALZERS 1 pc Own construction 1	All elements, local coordination chemical bond	0.1—10 ppm (depending on the element)	A few times 100 μm	$\simeq$5 nm	Heatable sample holder. Examination of depth profile
Reactive SIMS	BALZERS 1 pc	All elements, except oxygen. Semiquantitative analysis	0.01—1 ppm (depending on the element)	A few times 100 μm	$\simeq$5 nm	Semiquantitative observation of the variation of depth concentration. Detection of trace impurities
SAM	PHI 545 A Physical Electronics 1 pc	All elements, except H and He, chemical bond	$\simeq$1000 ppm	2—3 μm	$\simeq$1—2 nm	Quantitative analysis. Depth profile examinations. Pictures of lateral distrib. Topographic picture
X-ray fluorescence analyzer	DRON — 2	Crystal orientation. Phase analysis. Grain dimension. Fluorescence analysis	For crystal orientation $\simeq$0.05°			Examination of mechanical stress
Microsonde	Under delivery					
Atom absorption spectrometer	AAS — 1 Carl Zeiss Jena	Composition of fluids	0.01 ppm			Examination of electroplaters. Examination of the composition of solid layers after introduction into fluids
Talystep equipment	In cooperation with the Department of Electronic Devices at the TUB	Depth measurements				
Metal microscope	Neophot — 2	Examination of all materials suitable for light reflection				Measurement of lateral microhardness

Nowadays there is sufficient international experience to support the statement that all these requirements cannot be met by a single analytical method.

The problems can be solved however, by the joint or often alternative application of the methods: SAM (scanning Auger electron spectroscopy), SIMS (secondary ion mass spectrometry), the electron microprobe method and, in some special cases the RBS (Rutherford back-scattering) and ESCA (X-ray photo electron spectrometry) associated with the previous ones. The home topicality of the problem is indicated by the increasing frequency of the metallurgic tasks outlined above (due to the qualitative development of our home metallurgy) and also by the actual availability of all the preconditions to create analytical instruments satisfying the above requirements [3]. In the Laboratory of Surface Physics of the Physical Institute at the Technical University, Budapest, national basis laboratory for local fine analysis, the following methods are at disposal (Table 1).

The photography of the instruments SIMS and SAM is shown in Fig. 1.

The lateral resolution of SAM is illustrated by the element distribution picture of Fig. 2. The examinations were carried out with the use of a photo-lithographed lateral resolution pattern. The distribution of the Si on the surface is seen. The real dimensions of the test area are 800 μm $\times$ 600 μm. A line thickness of 2.8 to 3.2 μm can still be distinguished on the photo.
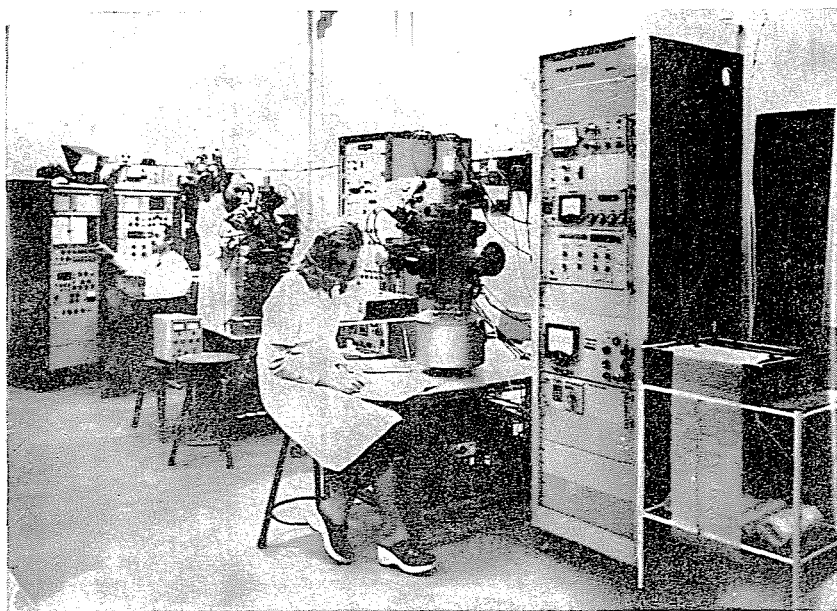

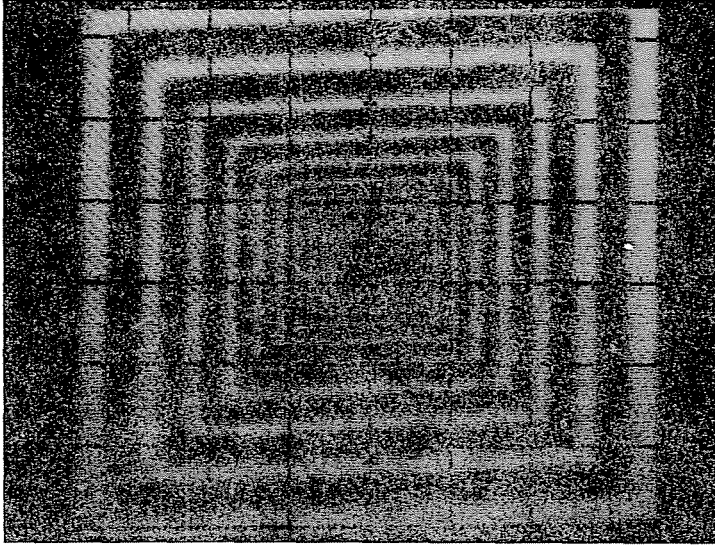*Fig. 1.* The SIMS and SAM instruments

Fig. 2. Silicon distribution on the lateral resolution pattern (enlarged $100 \times$)
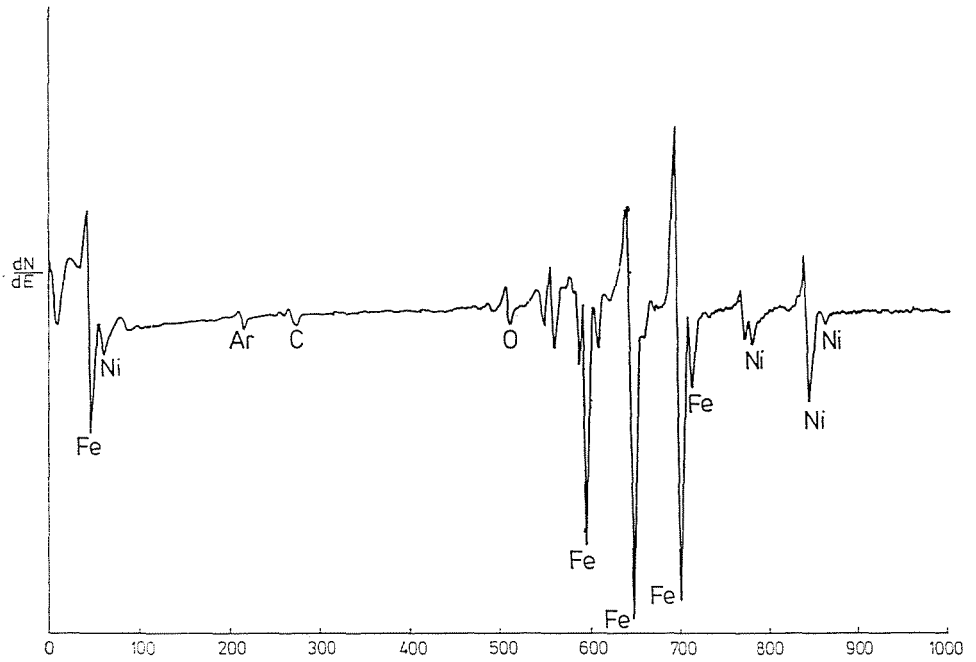

Fig. 3. Auger electron energy spectrum of a Fe—Ni standard alloy sample

A measurement series was made to check the quantitativenes of the SAM method. Eight samples of Fe—Ni alloy of different compositions were examined, where the Ni was increasing from about 10 at. % to 80 at.% in increments of approximately 10 at.%. To eliminate the local inhomogeneities of the samples, the diameter of the primary electron beam was chosen to 500 μ, and then an Auger electron energy spectrum was recorded from each sample. One of the spectra is shown in Fig. 3.

Table 2

Sample No.	Ni (nm) $S_z=0.26$	Fe (nm) $S_z=0.21$	Reduced peak			Measured Ni con-centration at. %	Atom abs. concentra-tion Ni at. %	Deviation of concen-tration at. %
			Ni	Fe	sum			
1	20	137	76.92	652.38	729.3	10.5	10.6	0.1
2	42	135	161.53	642.85	804.4	20.1	20.7	0.6
3	74	132	284.62	628.57	913.19	31.2	31.6	0.4
4	121	133	465.38	633.33	1098.72	42.4	41.0	1.4
5	149	116	573.08	552.38	1125.46	50.9	50.0	0.9
6	138	68	530.77	323.81	854.58	62.1	60.5	1.6
7	138	44	530.77	209.52	740.29	71.7	70.5	1.2
8	139	28.5	534.62	135.71	670.33	79.7	79.5	0.1

The Ni — concentrations accepted as standards were established by the method of atom absorption. The measurement results and data are contained in Table 2. The greatest deviation between the analytical data and measured concentrations was 1.6%. It is to be noted that the calculation of the quan-titative values neglected the impurities (e.g., Ar, O, C) of small concentration present on the sample surfaces. S_x is the relative sensitivity factor.

II. Results of local and distribution measurements on metals

In the following sections, the efficiency of local distribution analysis will be illustrated through examples essential for and interesting from the point of view of the non-ferrous, aluminium, tungsten and steel industries.

Examination of aluminium alloys. The results of various measurement methods on samples taken from aluminium metal baths are summarized in Table 3. The measurement methods were: neutron activation analysis, SIMS and SAM.

Table 3

Sample No.	Oxygen concentration (neutron act. an) [PPM]	Results of the SIMS investigations (relative O conc.)					SAM investigations O conc. [at. %]
		$\langle Al^+\rangle$	$\langle \Delta Al^+\rangle$	$\langle O^-\rangle$	$\langle \Delta O^-\rangle$	$\dfrac{\langle O^-\rangle}{\langle Al^+\rangle}$	
1	14	$2.6 \cdot 10^4$	$0.35 \cdot 10^4$	$4.3 \cdot 10^3$	$1.8 \cdot 10^3$	0.16	homogeneous part $<0.1\%$ inhomogeneous part $\simeq 1\%$
2	13.7	$2.9 \cdot 10^4$	$0.87 \cdot 10^4$	$4.5 \cdot 10^3$	$1.4 \cdot 10^3$	0.15	homogeneous part $<0.1\%$ inhomogeneous part $\simeq 1\%$
3	200.0	$2.8 \cdot 10^4$	$0.63 \cdot 10^4$	$6.1 \cdot 10^3$	$4.1 \cdot 10^3$	0.22	homogeneous part 0.4% inhomogeneous part 6.3%

The examinations aimed at determining the oxide content and the lateral inhomogeneity of the samples. As an analysis with neutron activation supplies data on the bulk composition, also in the SIMS measurements it was desirable to obtain depth data exempt from surface effects. Therefore the SIMS spectra underlying the evaluation were recorded after considerable sputtering, when the depth profile curves of the components had reached their stationary values. With some samples, spectra were prepared at about 8 to 10 surface points. The $\langle Al^+\rangle$ and $\langle O^-\rangle$ averages calculated from the spectra are contained in the Table, with indications of the standard deviations.
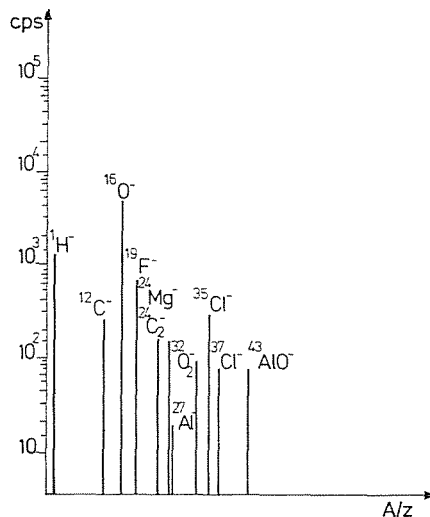

Fig. 4. Negative secondary ion spectrum of an aluminium sample in the mass range of 0 to 100 a.m.u.

The variation of the relative oxygen content $\langle O^-\rangle/\langle Al^+\rangle$ pertaining to the different samples is seen to exhibit a nature similar to that obtained with activation analysis.

This observed tendency is supported also by Auger measurements. The samples examined were found laterally inhomogeneous. The SAM measurements revealed several oxide enrichments of a size of some 10 μm on the sample surfaces. A negative secondary ion mass spectrum made on such an enrichment with considerable peaks of $^{16}O^-$ and $^{43}AlO^-$ is shown in Fig. 4.

Also Auger element distribution pictures were recorded from sample surface spots with oxygen enrichment. The oxygen, aluminium and copper distributions are seen in Figs 5, 6 and 7, respectively. In the place of oxygen enrichment the aluminium content decreases, but copper, a fine impurity, accumulates. The inhomogeneities seen in the figures have a size of about 20 μm.

As a conclusion of the above examinations it can be stated that the measuring methods applied are suitable for the local and distribution analysis of aluminium alloys.

Examination of a Cu—Co—Si alloy. A copper alloy containing 0.36 percent by weight of Co and 0.11 percent by weight of Si melted by the vacuum induction method and cast into a rod, then forged to 16 mm and pulled to
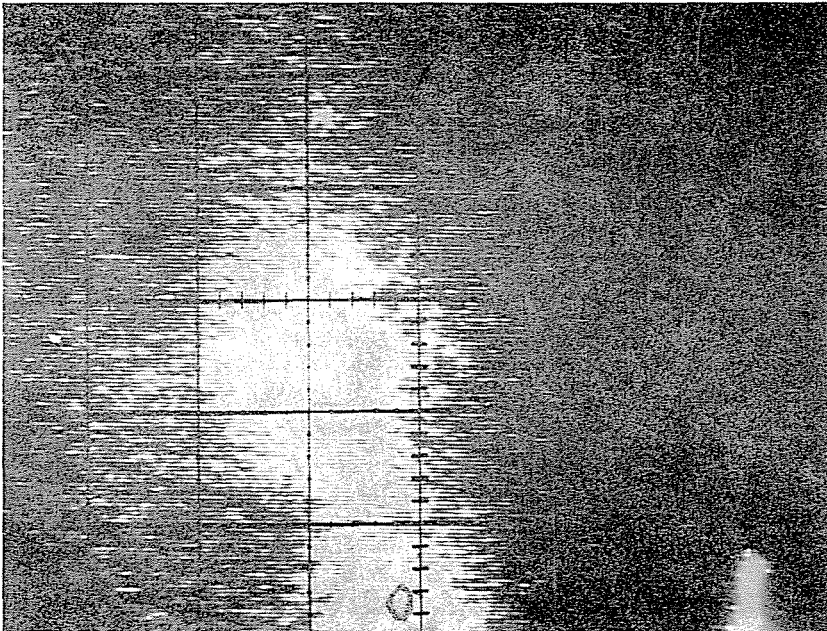
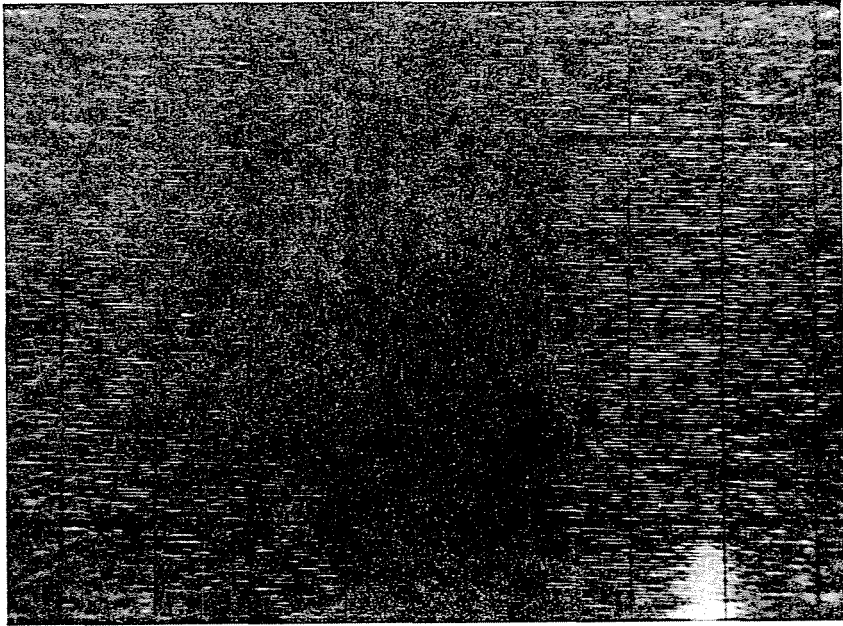*Fig. 5.* Oxygen distribution on the surface of an aluminium sample (enlarged 1000 ×)

Fig. 6. Aluminium distribution on the surface of an aluminium sample (enlarged 1000×)

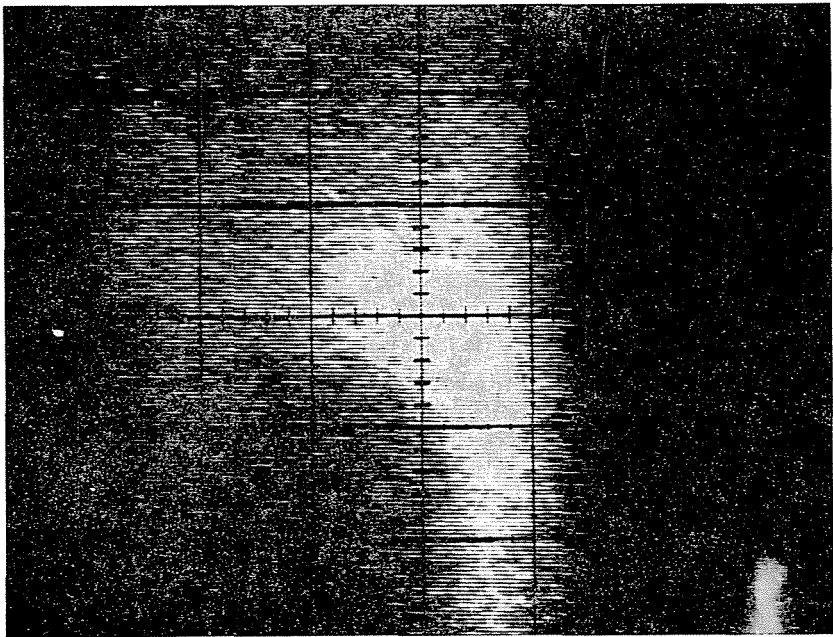*Fig. 7.* Place of enrichment of impurity (Cu) on the surface of an aluminium sample (enlarged 1000×)

14 mm was examined. Prior to examination, the sample was subjected to heat treatment at 900 °C for 1 hour, then, after cooling down, to a post--treatment of one hour at 600 °C.

To have a surface layer examinable at full depth, an about 15 mm long sample piece was milled wedge-shaped. The milled surface was polished by diamond paste.

The sample was examined by the SIMS method on 8 surface portions. In each measurement place the layer (of about 500 nm) destructed during polishing was removed by sputtering. After this, positive and negative secondary ion spectra were recorded. Fig. 8 shows a negative secondary ion spectrum. At mass number 87, cluster ion was detected, identified as cobalt-silicide.

The profile curves of Fig. 9 illustrate relative concentration variations arisen in the surface layer of the alloy sample. The oxygen content is seen to exceed in a 0.45 mm thick surface layer by more than one order of magnitude that inside the sample. Also the silicon ion intensity increases on the surface, but a part of the increase can be ascribed to the increase of the ion yield connected with the higher oxygen content of the surface. In a depth of 0.45 mm from the original surface, a slight impoverishment in silicon could be observed. The silicon oxide had its maximum intensity on the surface. Adjacent to the surface, an enrichment in cobalt-silicide could be detected.
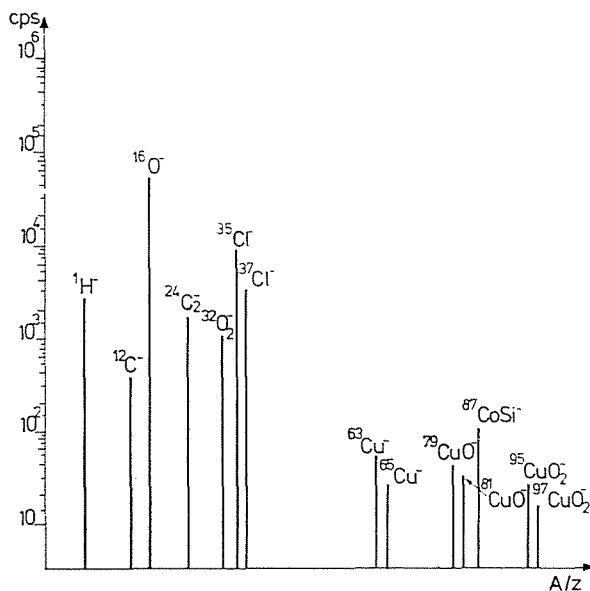

Fig. 8. Negative secondary ion spectrum of a Cu—Co—Si alloy in the mass range of 0 to 100 a.m.u.
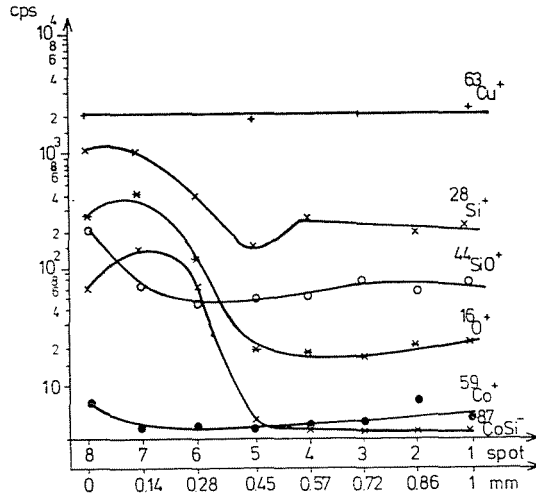
Fig. 9. Distribution of the depth concentration of components in a Cu—Co—Si alloy sample

The surface of the Cu—Co—Si was examined also by means of scanning Auger electron spectroscopy (SAM).

The Si distribution is seen in Fig. 10 taken with a 250-fold magnification and showing considerable Si-enrichments.
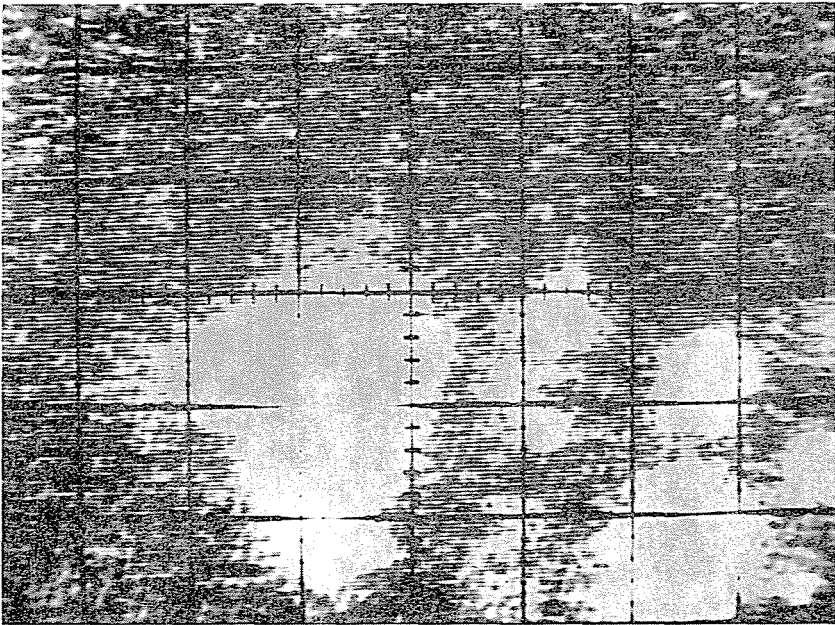

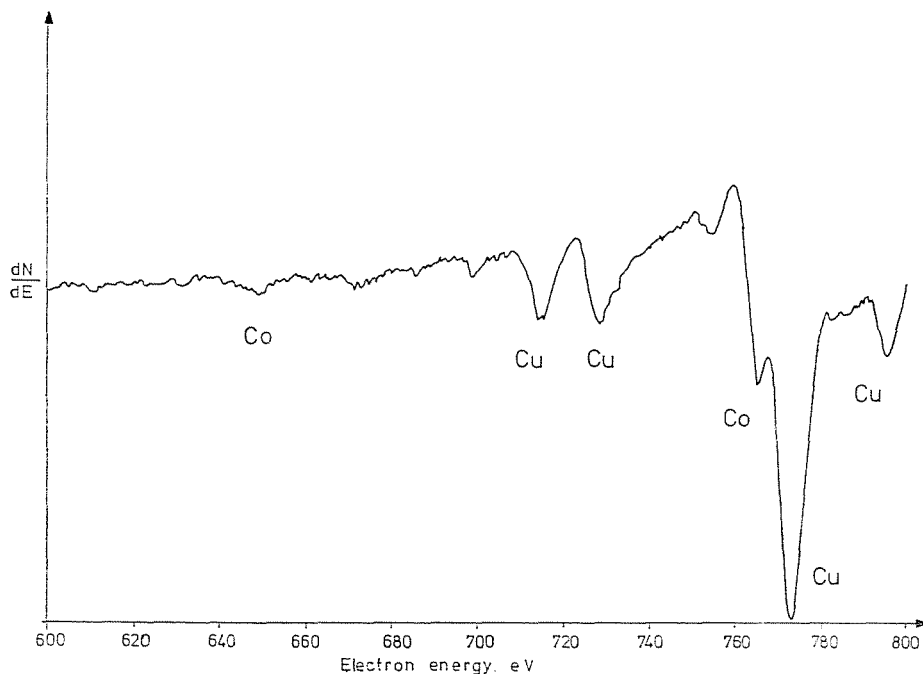*Fig. 10.* Silicon distribution (enrichment) in a Cu—Co—Si alloy (enlarged 250×)

Fig. 11. Auger electron energy spectrum (in a place of silicon enrichment) of a Cu—Co—S alloy sample

The Auger electron energy spectrum shown in Fig. 11 was recorded from the middle of the largest Si precipitation seen in Fig. 10. The Co peak appears here shifted by a few eV. As a comparison, Fig. 12 shows a spectrum made from a homogeneous part of the sample under similar measurement conditions. There is no energy peak here that could be identified as cobalt.

Thus the observed joint enrichment of Si and Co leads to the conclusion that in alloys of this type precipitates of cobalt-silicide may be found [4].

Beryllium bronze (Cu — 2% of Be, and Zr, Mg as alloying metals).

The SIMS and SAM examinations aimed at determining the composition of the layer formed on the surface of a beryllium bronze strip kept at 850 °C for an hour before being cooled down in water and difficult to remove by pickling.

The SIMS profile curves made by reactive sputtering have evinced that on the strip surface a thick surface layer (of about 1000 nm) with a composition differing from that inside the strip develops, with a much higher relative concentration of the alloying beryllium (Fig. 13).

Part of the beryllium enriched on the surface is bonded with oxygen (BeO, BeO_2, etc.) with Cu/(CuBe) and with microalloying components (BeZr) as indicated by the cluster ions seen in the spectrum of Fig. 14. Also the Auger
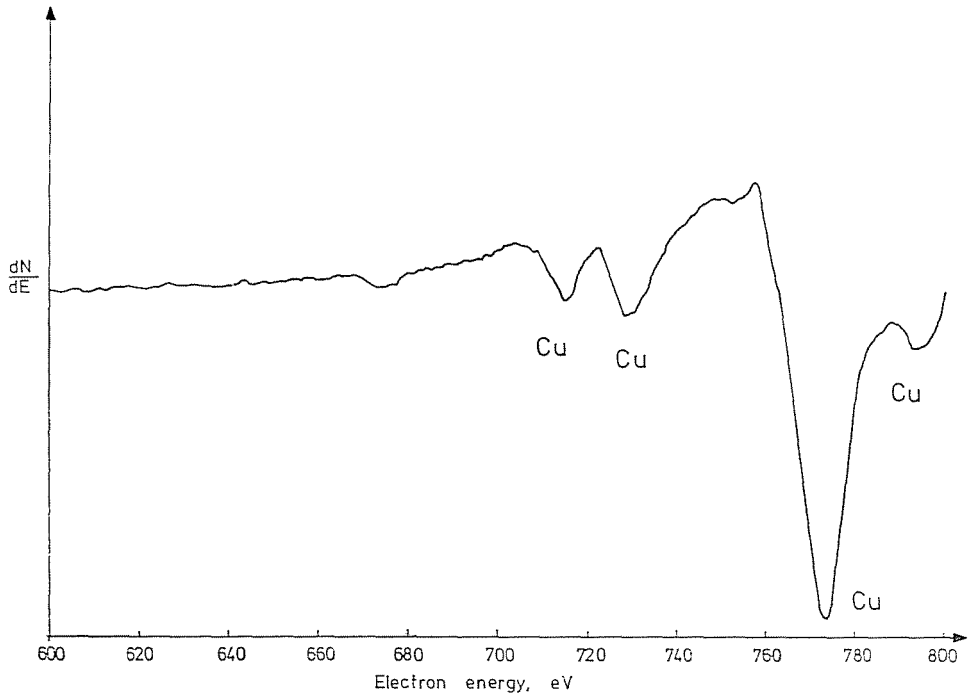
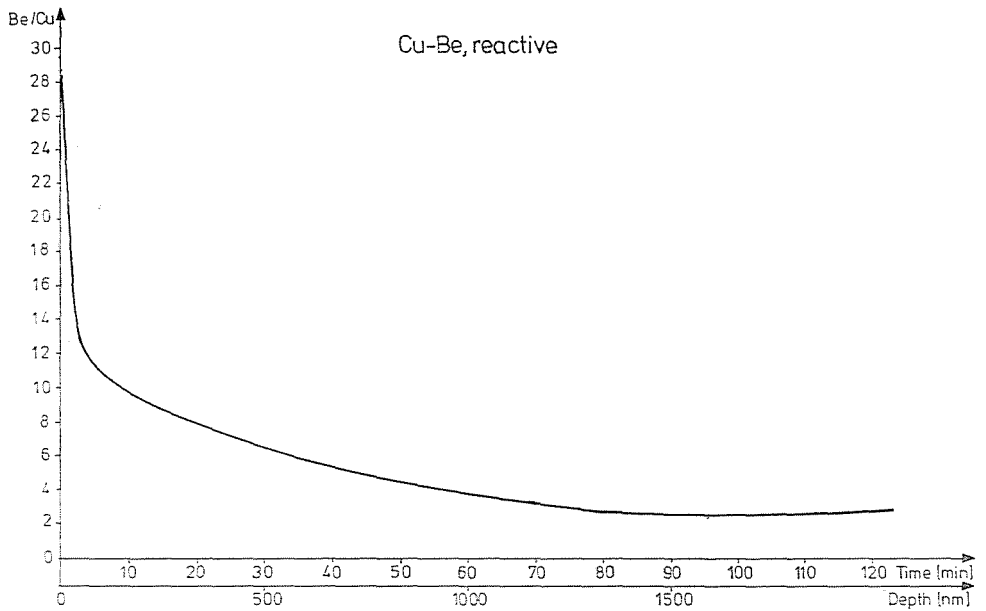*Fig. 12.* Auger electron spectrum of a Cu—Si—Co alloy sample (on a silicon surface region)

Fig. 13. Depth concentration distribution of the beryllium component of a sample of beryllium bronze (Cu—2% of Be)
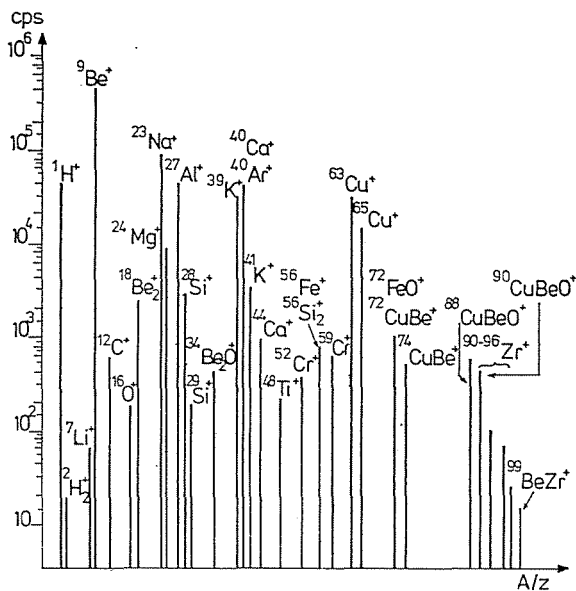
Fig. 14. Positive secondary ion spectrum of a sample of beryllium bronze (Cu — 2% Be, Zr, Mg microalloying) in the mass range of 1 to 100 a.m.u.
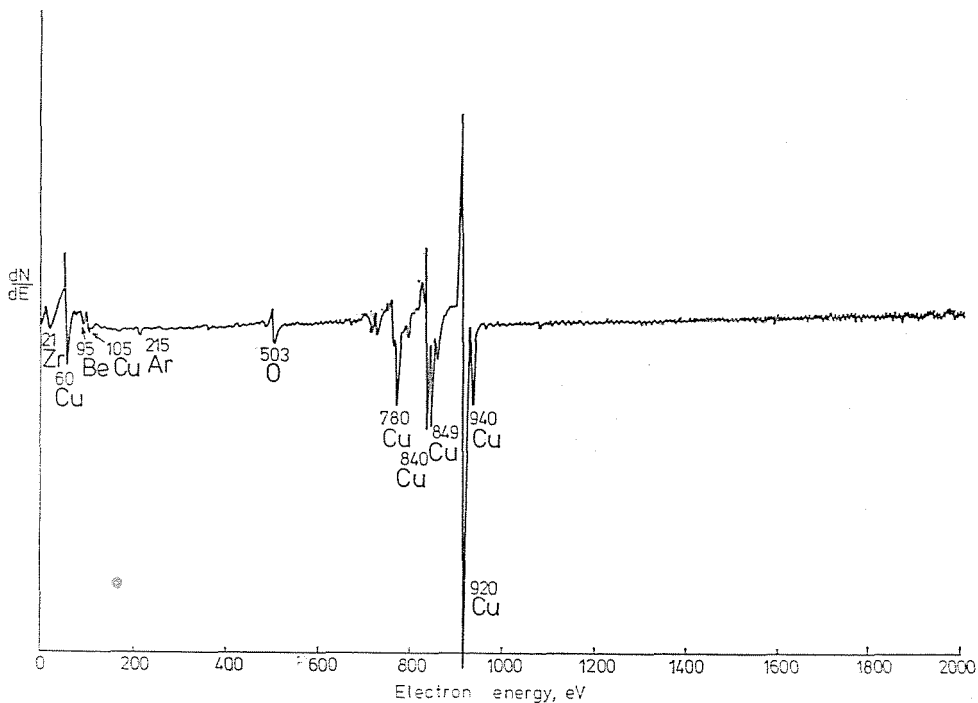

Fig. 15. Auger electron spectrum of a beryllium bronze (Cu — 2% Be) sample
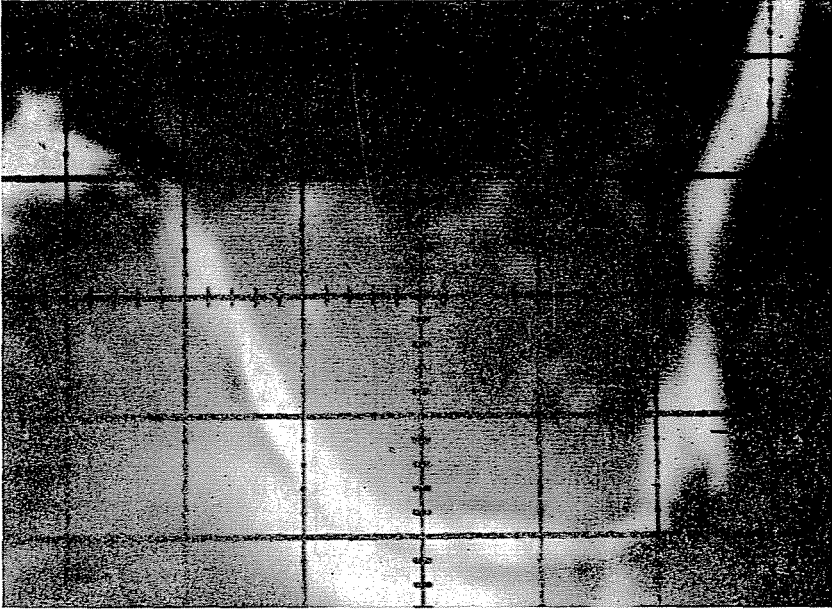
3*

Fig. 16. Absorbed current picture (ABS) made from the surface of a beryllium bronze (Cu —
—2% Be, Zr, Mg microalloying) alloy sample

Fig. 17. Copper distribution in a beryllium bronze (Cu — 2% Be, Zr, Mg microalloying)
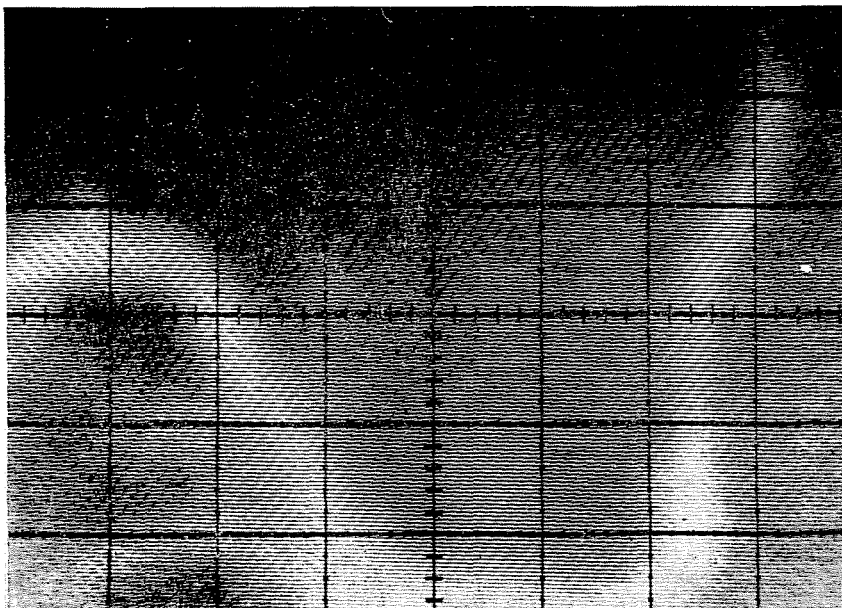alloy sample (enlarged 250 ×)

Fig. 18. Zirconium distribution in a beryllium bronze (Cu — 2% Be, Zr, Mg microalloying) alloy sample (enlarged 250×)
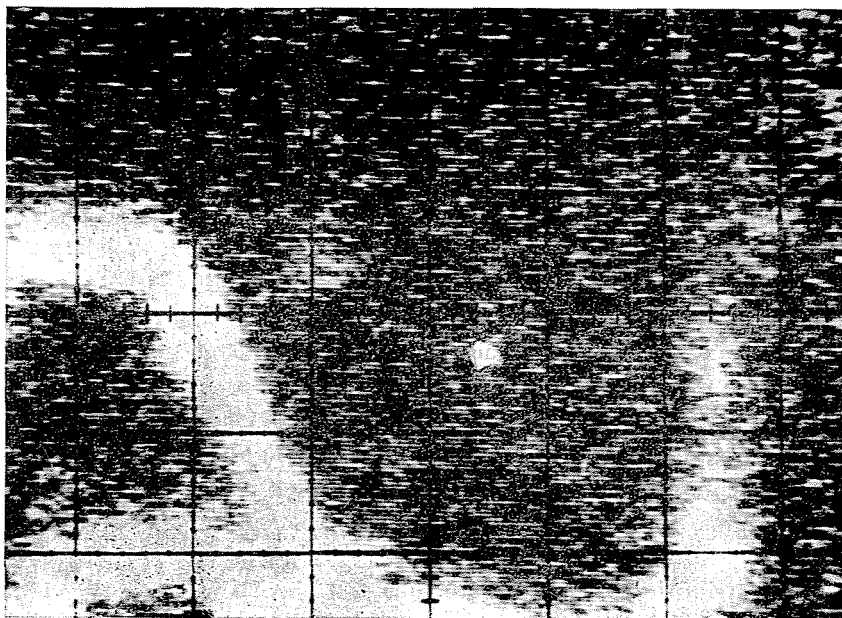

Fig. 19. Distribution picture made from a characteristic oxygen enrichment on a beryllium bronze (Cu — 2% Be, Zr, Mg mircroalloying) alloy sample (enlarged 250×)
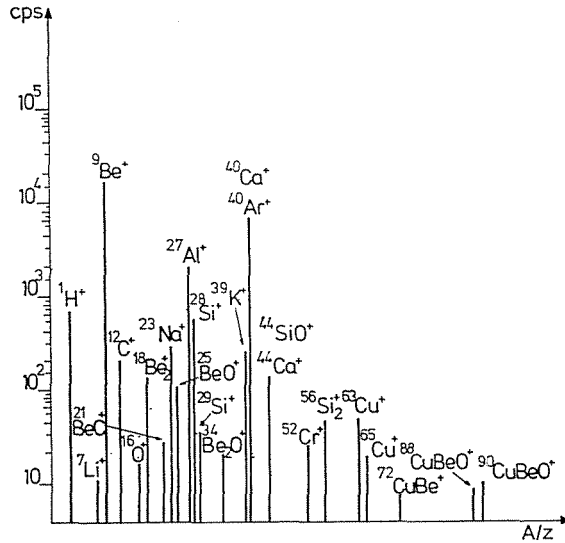
Fig. 20. Positive secondary ion spectrum recorded from a beryllium bronze (Cu — 2% Be) alloy sample containing carbon, impurity, in the mass range of 0 to 100 a.m.u.

energy spectrum of Fig. 15 demonstrates that a part of beryllium is in bonded state, i.e. it appears at 95 eV instead of 105 eV, owing to the chemical shift. The significant lateral inhomogeneity of the surface layer is illustrated by the topographic picture shown in Fig. 16.

The characteristic element distribution of surface inhomogeneity is shown in Figs 17, 18 and 19. The regions of inhomogeneity appear partly as impoverishments in copper, partly as enrichments in oxygen and zirconium.

The above examinations supplied data to the modification of the pickling procedure.

Also the surface of beryllium bronze preproduct produced by horizontally controlled crystallization was examined in cases when the alloy adhered to the graphite mould. In the surface layer of such strips large amounts of free carbon as well as carbon bonded to beryllium (BeC) were detected (Fig. 20) and, at the same time, also the surface enrichment of beryllium was more marked. These examinations pointed out the unfitness of graphite mould for a controlled crystallization of the beryllium bronze.

In the examination of *FeB metal glass samples* the problem arises whether the composition before annealing decomposes to iron, ferric boride and boron. Figs 21, 22, 23 show the distribution pictures of Fe, B and O, respectively.

The distribution pictures show places to exist where iron and boron impoverish or enrich together. In such regions iron and boron are likely to be bonded to each other. Apart from these places, in the right lower section
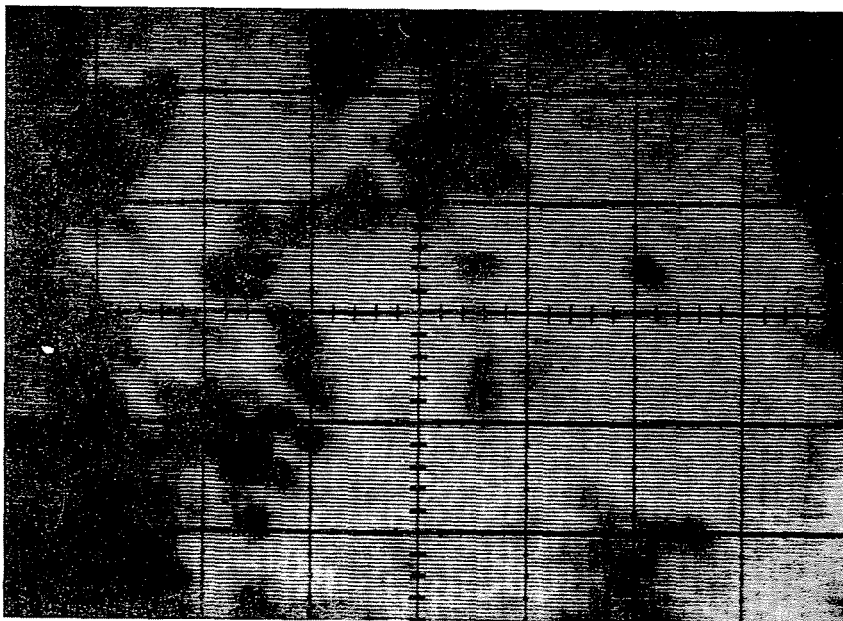
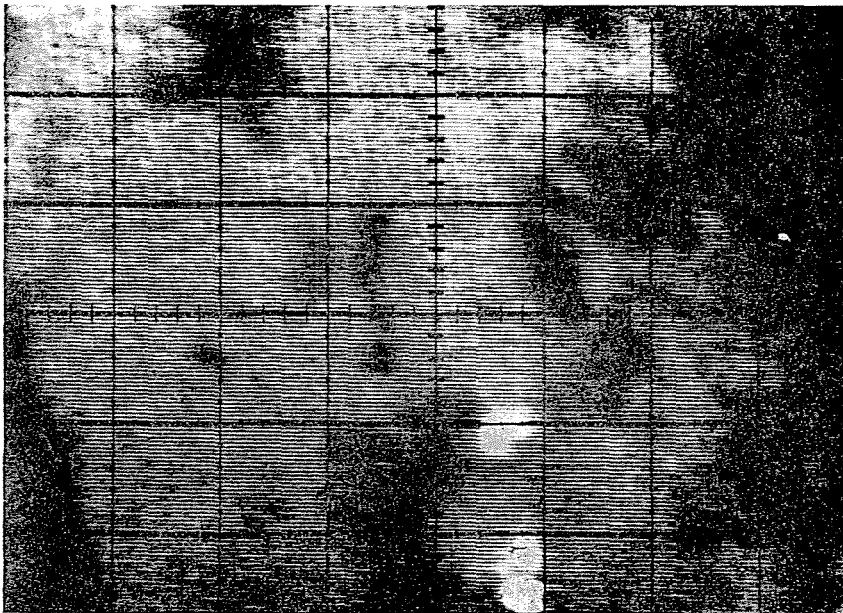*Fig. 21*. Iron distribution in an iron — boron metal glass sample (enlarged 100×)

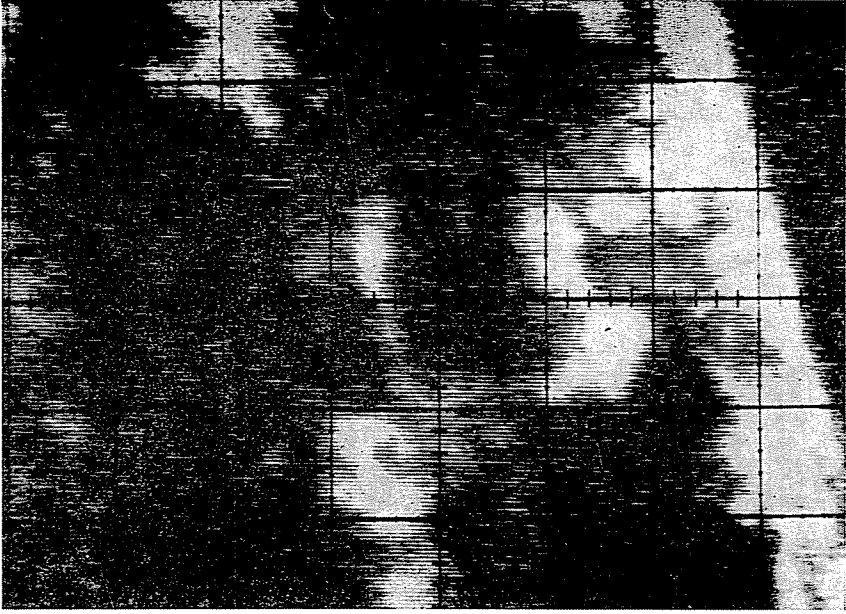*Fig. 22*. Distribution of boron in an iron—boron metal glass sample (enlarged 100×)

Fig. 23. Oxygen distribution in an iron—boron metal glass sample (enlarged 100×)
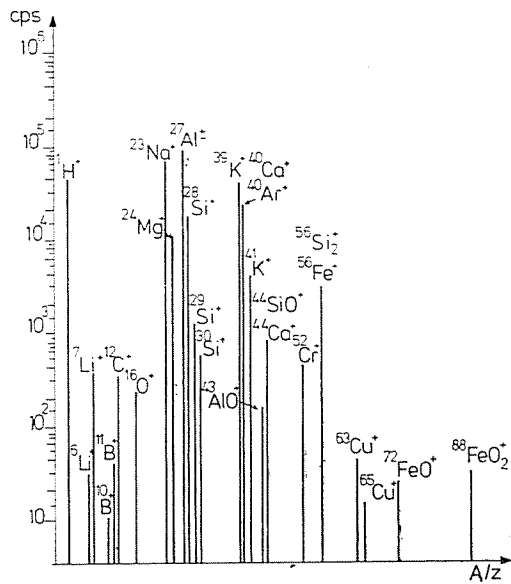

Fig. 24. Positive secondary ion spectrum recorded from the cross section of a sintered tungsten rod, in the mass range of 0 to 100 a.m.u.
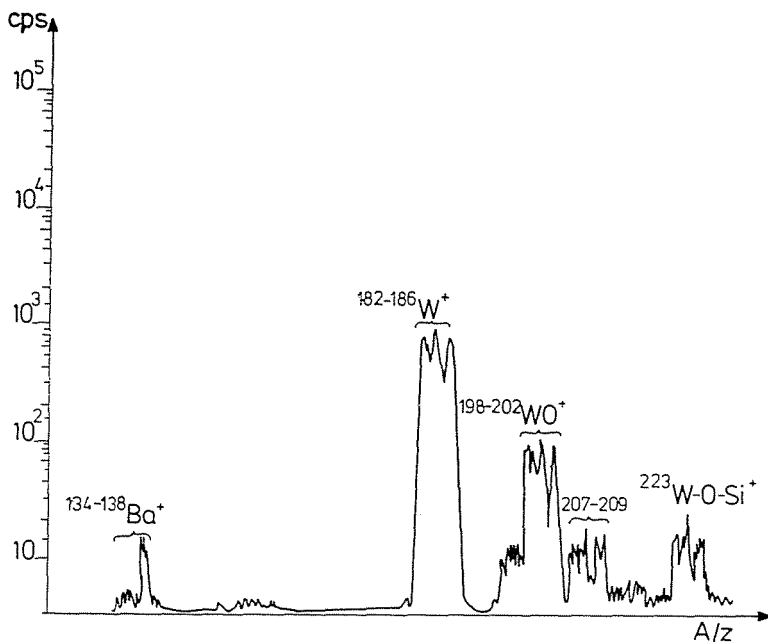
Fig. 25. Positive secondary ion spectrum recorded from the cross section of a sintered tungsten rod, in the mass range of 100 to 300 a.m.u.
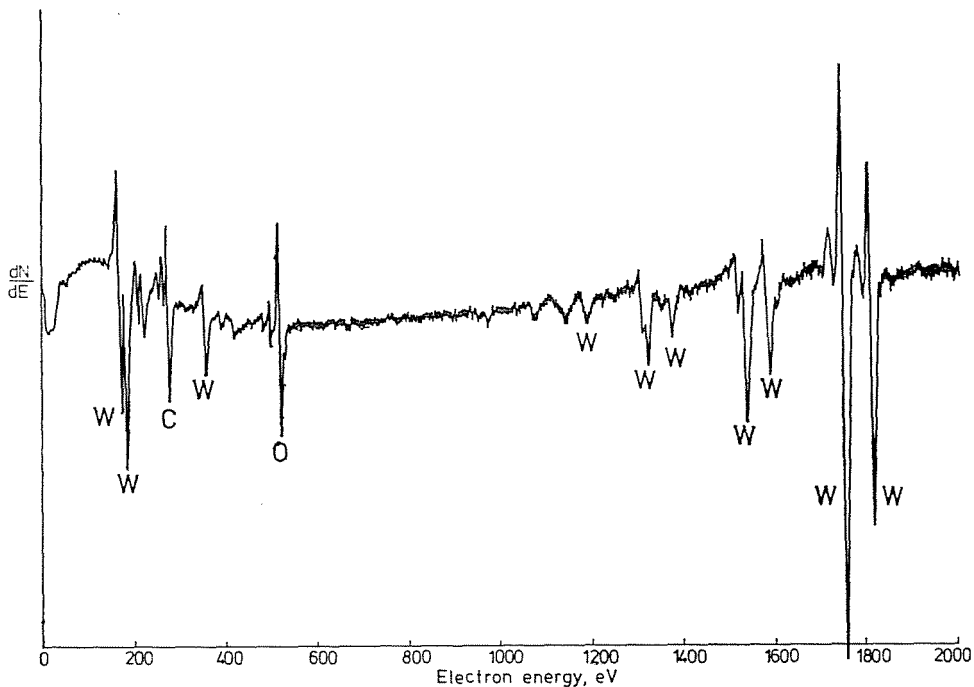

Fig. 26. Auger electron energy spectrum (on a homogeneous surface portion) recorded from the cross section of a sintered tungsten rod
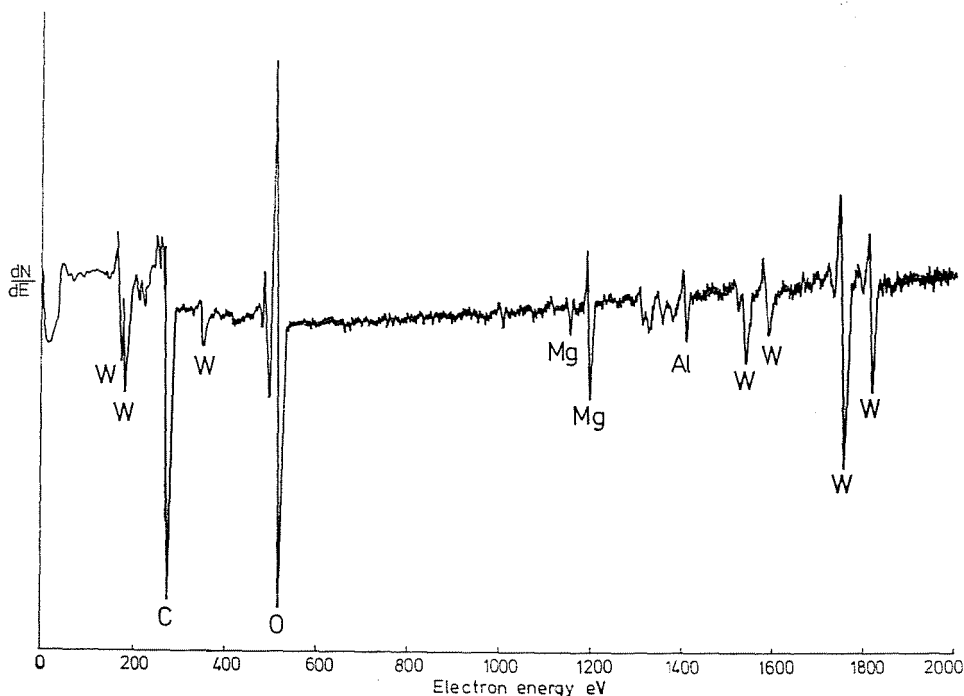
Fig. 27. Auger electron energy spectrum recorded from the cross section (across a surface inhomogeneity of a sintered tungsten rod)

of the distribution picture of boron, two considerable boron enrichments can be observed. On the other hand the distribution of iron is finer and less granulated than that of boron.

In this surface region a significant oxygen content was detected, the distribution of which was a counterpart to the iron distribution: where one of these elements enriches, the other impoverishes, and vice versa.

Sintered tungsten rod. Small amounts (a few 10 ppm) of potassium, aluminium or silicon additives have a favourable effect on the structure of tungsten spirals made from a sintered tungsten rod, but larger or unevenly distributed amounts of the additives produce a spurious effect. Such small amounts of additives or impurities can readily be detected by the SIMS method — as demonstrated by the secondary ion spectrum of Fig. 24. However, not only the additives or impurities themselves can be detected, but the appearing cluster ions ($^{198-202}WO^{+}$, $^{207-209}WC_2^{+}$ etc. in Fig. 25) refer to possible development of compounds. Such small amounts of homogeneously distributed additives or impurities cannot be detected by the Auger method (Fig. 26). On the other hand, their local enrichment can easily be observed also on the Auger energy spectrum, as illustrated by the electron energy spectrum in Fig. 27.

Summary

The requirements of the local and distribution analysis of metals and alloys are reviewed, and examples are given to demonstrate that the requirements can be met under Hungarian conditions.

The presented examples show the advantages of the complementary SIMS—SAM investigations. For instance, the chemical shift of the Co peak indicated by SAM and the CoSi$^-$ ions detected by SIMS refer to the evolution of CoSi precipitates. Similarly, the chemical shift of the Be peak can be understood by indicating cluster ions formed by Be with other materials such as O, Cu and Zr.

In the case of W, SIMS was used as a method for detecting dopants (K, Al, Si) in very small quantities (ppm range).

Also dopants (Al) of inhomogeneous distributions could be detected by SAM.

Other applications such as the detection of oxygen inhomogeneity in aluminium alloys and the distribution of components of metallic glasses (FeB type) are also of great practical importance.

References

1. KASSEL, K. R.: Aluminium, **37** 288 (1961)
2. KISSLING, R. J.—WALLACE, J. P.: Foundry, **91**, 70 (1963)
3. BERÉNYI, D.: New Methods of the Surface Examination of Solid Bodies. Recent Results of the Investigations of Solids (in Hungarian). Akadémiai Kiadó, Budapest, 1979
4. PAVLYÁK, F.—PERCZEL, I. V.—GIBER, J.: Surface and Interface Analysis, **1**, 139 (1979)

Prof. Dr. János GIBER
Józsefné PERCZEL
Ferenc PAVLYÁK
Béla ALBERT

H-1521 Budapest